# Electron-impact excitation of argon at intermediate energies

Oleg Zatsarinny,[1,*] Yang Wang,[1,2,†] and Klaus Bartschat[1,3,‡]
[1]*Department of Physics and Astronomy, Drake University, Des Moines, Iowa 50311, USA*
[2]*Center for Theoretical Atomic and Molecular Physics, Academy of Fundamental and Interdisciplinary Sciences, Harbin Institute of Technology, Harbin 150080, People's Repulic of China*
[3]*ITAMP, Harvard-Smithsonian Center for Astrophysics, Cambridge, Massachusetts 02138, USA*
(Received 8 January 2014; published 18 February 2014)

Large-scale $R$-matrix-with-pseudostates calculations for electron collisions with argon atoms, using a recently developed parallel version of our $B$-spline $R$-matrix code, are reported. The calculations were carried out in the semirelativistic $jK$-coupling scheme. They are intended to provide converged (with respect to the number of coupled states) results for electron-impact excitation of individual target states with dominant configurations $3p^54s$, $3p^54p$, $3p^53d$, and $3p^55s$ for incident electron energies from threshold to 300 eV. The close-coupling expansion includes 500 target states, with the lowest 78 states representing the bound spectrum and the remaining 422 the ionization continuum. The results reveal dramatic reductions of the predicted excitation cross sections at intermediate energies due to a strong influence of coupling to the target continuum and the higher-lying Rydberg states. Comparison with available experimental data for excitation raises questions about the absolute normalization in the measurements.

DOI: 10.1103/PhysRevA.89.022706 PACS number(s): 34.80.Dp

## I. INTRODUCTION

Electron-impact excitation of noble gases, argon in particular, has many applications in different areas such as gaseous electronics, astrophysics, and controlled nuclear fusion. Not surprisingly, therefore, a recent work was devoted to a thorough assessment of currently available experimental and theoretical data for electron-Ar [1], electron-He/Ne [2], and electron-Kr/Xe [3] collisions, as well as a summary of theoretical methods frequently used for the calculations [4]. Specifically, the papers referenced above concentrated on the data currently available in the LXcat database [5]. We refer in particular to [1] for an extensive list of references to experimental and theoretical work on electron-Ar collisions.

The purpose of the present paper is to provide a detailed account of our calculations for angle-integrated elastic, momentum-transfer, excitation, and ionization cross sections for electron-Ar collisions. While many of our final results are publicly available through LXcat [5], only a very brief description has been given before. In particular, the very important aspect of convergence with respect to the number of states retained in the close-coupling expansion, a crucial issue in any assessment of the accuracy of our predictions, has not been addressed yet.

In Sec. II we briefly summarize our computational model. This is followed in Sec. III by a comparison with a variety of experimental data for angle-integrated cross sections. Specifically, we will discuss elastic scattering, including the momentum-transfer cross section (Sec. IIIA), excitation (Sec. IIIB), ionization, including ionization from the metastable initial states, and the grand total cross section (Sec. IIIC). A qualitative explanation for the features seen in the calculation will be given in Sec. IIID. We finish with a short summary and conclusions in Sec. IV.

## II. COMPUTATIONAL DETAILS

The target-structure calculations and the scattering calculations in the present work are very similar to our recent $R$-matrix-with-pseudostates (RMPS) calculations for electron-Ne collisions [6,7]. The target states were generated by combining the multiconfiguration Hartree-Fock and the $B$-spline box-based multichannel methods [8]. We include the $3s^23p^5nl$ and $3s3p^6nl$ Rydberg series of bound states in Ar, as well as continuum pseudostates lying above the ionization limit. Inner-core (short-range) correlations are represented through the configuration-interaction expansion of the corresponding ionic states. We employ the Breit-Pauli Hamiltonian to account for relativistic effects, which manifest themselves predominantly in a large spin-orbit mixing of different $LS$ terms.

In our atomic-structure calculations for noble gases [9], we found that core-valence correlation corrections are important for an accurate representation of the excited $3p^5nl$ states and this correlation can be taken into account by including core-excited configurations. That was indeed done in our $B$-spline $R$-matrix (BSR) calculations BSR-31 [10] for electron-Ar collisions and resulted in very accurate excitation energies of the target states included in the close-coupling expansion. In the present calculations with many more states, we decided to omit the core-valence correlation since it would have doubled the size of the target expansions and made the subsequent scattering calculations too extensive. The present expansions in $jK$-coupling contained between 50 and 80 configurations for each state. Although still a challenge, such expansions can be handled with our available computational resources in the subsequent large-scale collision calculations. As seen from Table I, the excitation energies for all physical bound states differed by no more than 0.2 eV from experiment. This

*oleg.zatsarinny@drake.edu
†yangwang0624@foxmail.com
‡klaus.bartschat@drake.edu

 

TABLE I. Energy levels of the most relevant discrete Ar levels for the present work, their respective thresholds for excitation from the ground state, and the difference between experiment [11] and the present theoretical description.

| State | Theory (a.u.) | Theory (eV) | Expt. (eV) | Diff. (eV) |
|---|---|---|---|---|
| $(3p^6)^1S_0$ | −528.7225512 | 0 | 0 | 0.000 |
| $4s[3/2]_2$ | −528.2919564 | 11.717 | 11.548 | 0.169 |
| $4s[3/2]_1$ | −528.2891267 | 11.794 | 11.624 | 0.170 |
| $4s'[1/2]_0$ | −528.2854885 | 11.893 | 11.723 | 0.170 |
| $4s'[1/2]_1$ | −528.2816298 | 11.998 | 11.828 | 0.170 |
| $4p[1/2]_1$ | −528.2457622 | 12.974 | 12.907 | 0.067 |
| $4p[5/2]_3$ | −528.2398823 | 13.134 | 13.076 | 0.058 |
| $4p[5/2]_2$ | −528.2390371 | 13.157 | 13.095 | 0.062 |
| $4p[3/2]_1$ | −528.2372363 | 13.206 | 13.153 | 0.053 |
| $4p[3/2]_2$ | −528.2363911 | 13.229 | 13.172 | 0.057 |
| $4p[1/2]_0$ | −528.2328264 | 13.326 | 13.273 | 0.053 |
| $4p'[3/2]_1$ | −528.2327896 | 13.327 | 13.283 | 0.044 |
| $4p'[3/2]_2$ | −528.2320179 | 13.348 | 13.302 | 0.046 |
| $4p'[1/2]_1$ | −528.2311359 | 13.372 | 13.328 | 0.044 |
| $4p'[1/2]_0$ | −528.2255500 | 13.524 | 13.480 | 0.044 |
| $3d[1/2]_0$ | −528.2080939 | 13.999 | 13.854 | 0.145 |
| $3d[1/2]_1$ | −528.2076529 | 14.011 | 13.854 | 0.157 |
| $3d[3/2]_2$ | −528.2069547 | 14.030 | 13.903 | 0.127 |
| $3d[7/2]_4$ | −528.2051540 | 14.079 | 13.979 | 0.100 |
| $5s[3/2]_2$ | −528.2046027 | 14.094 | 14.013 | 0.081 |
| $3d[7/2]_3$ | −528.2045660 | 14.095 | 14.063 | 0.032 |
| $5s[3/2]_1$ | −528.2040515 | 14.109 | 14.068 | 0.041 |
| $3d[5/2]_2$ | −528.2032430 | 14.131 | 14.090 | 0.041 |
| $3d[5/2]_3$ | −528.2028387 | 14.142 | 14.099 | 0.043 |
| $3d[3/2]_1$ | −528.2009645 | 14.193 | 14.153 | 0.040 |
| $5s'[1/2]_0$ | −528.1991638 | 14.242 | 14.214 | 0.028 |
| $5s'[1/2]_1$ | −528.1985023 | 14.260 | 14.234 | 0.026 |
| $3d'[5/2]_2$ | −528.1982450 | 14.267 | 14.236 | 0.031 |
| $3d'[3/2]_2$ | −528.1980245 | 14.273 | 14.241 | 0.032 |
| $3d'[5/2]_3$ | −528.1978408 | 14.278 | 14.255 | 0.023 |
| $3d'[3/2]_1$ | −528.1961503 | 14.324 | 14.304 | 0.020 |

is considered sufficiently accurate for intermediate-energy scattering calculations, i.e., when the projectile energy is relatively far away from the near-threshold resonance regime.

Another assessment of the quality of our target description can be obtained by comparing the results for the oscillator strengths. For the principal resonance transitions from the ground state to the $3p^54s'[1/2]_1$ and $3p^54s[3/2]_1$ states, for example, our oscillator strengths are 0.0634 and 0.262, respectively, and agree well with the experimental data [12]. This is important for absolute normalization of the angle-integrated excitation cross section for these transitions at high energies. A more detailed comparison of available experimental and theoretical data for the oscillator strength was given earlier [9] and will not be repeated here. Even though the present target expansions are significantly smaller than those employed in [9], they still provide quite accurate results, thus indicating that principal correlation corrections have been accounted for.

Finally, the electric dipole polarizability is a very important parameter in the description of elastic scattering at very low energies. The present expansion yields a ground-state polarizability of $10.74a_0^3$, which is very close to the experimental value of $11.07a_0^3$ [13].

The scattering calculations were carried out in the framework of the $R$-matrix method. We employed a recently developed, fully parallelized version of the BSR complex [14]. The $R$-matrix radius was set to $25a_0$, where $a_0 = 0.529 \times 10^{-10}$ m is the Bohr radius. We employed 65 $B$-splines to span this radial range using a semiexponential grid of knots. The maximum interval in this grid is $0.5a_0$, which is sufficient for electron scattering energies up to 300 eV. We calculated partial waves for total electronic (spin plus orbital) angular momenta $J \leqslant 50.5$ numerically and then used a top-up procedure to estimate the contribution to the transition matrix elements from even higher $J$ values. The calculation for the external region was performed with the STGF program [15].

The close-coupling expansion for our final results includes 500 states of argon, with the lowest 78 states representing the bound spectrum and the remaining 422 the target continuum. We included all $3s^23p^5nl$ and $3s3p^6nl$ states with $l = 0$–3. This model will be referred to as BSR-500 below. The continuum pseudostates in the present Breit-Pauli model cover the energy region up to 45 eV. This scattering model contained up to 2462 scattering channels. For a given $B$-spline basis, this number defines the size of the matrices involved. In the present work it leads to generalized eigenvalue problems (for each partial-wave symmetry) with matrix dimensions up to 150 000. This is essentially the limit that can be handled with our current computational resources.

In order to check the convergence of our results with respect to the number of states included in the close-coupling expansion, we also carried out a number of other calculations, including only the lowest 5 or 31 physical target states (below these models will be referred to as BSR-5 and BSR31, respectively), all (physical and pseudo) states with excitation energies below the first ionization threshold (BSR-78), a model with these 78 states and an additional 82 pseudostates with energies in the ionization continuum (BSR-160), and finally an even larger model with a total of 600 states. Due to the enormous computational resources required for the latter calculation, it was only carried out for a few selected energies up to 50 eV incident energy (using less basis splines) in order to assess the likely level of convergence in the BSR-500 results.

## III. RESULTS

### A. Elastic scattering

Figures 1 and 2 show the elastic and momentum-transfer cross sections over a wide range of incident electron energies between a few meV and several hundred eV. Over the years, several experiments have been carried out and many other calculations were performed for comparison. Many of the numerical models were designed to treat elastic scattering and hence it is not surprising that the overall agreement between experiment and theory is generally satisfactory (see, for example, [1] for detailed comparisons and also Fig. 2 below). It is however worth noting that our BSR approach can handle the entire energy range with a *single* approach, which is also used to treat the excitation and ionization processes discussed in the following subsections.

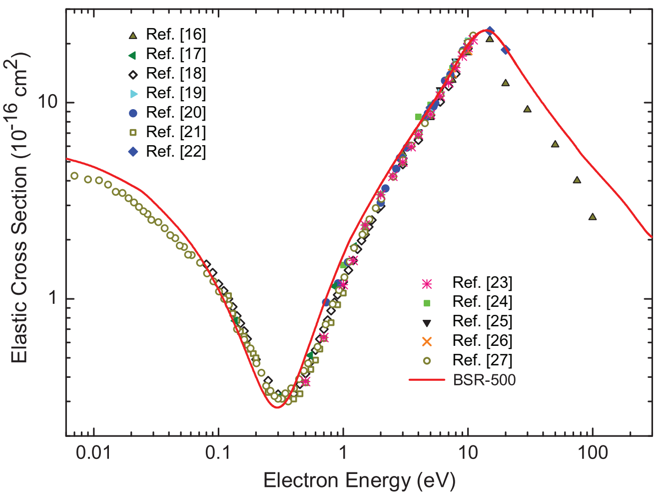


FIG. 1. (Color online) Angle-integrated cross section for elastic electron scattering from argon atoms in their $(3p^6)^1S_0$ ground state. The current BSR-500 results are compared with a variety of experimental data [16–27] indicated in the legend.

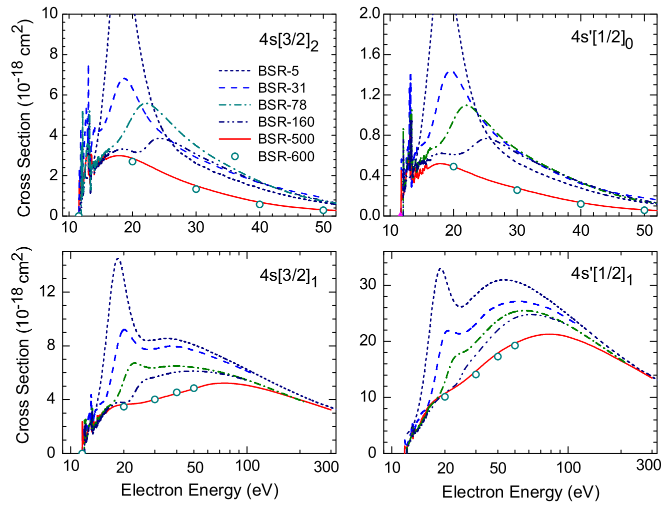


FIG. 3. (Color online) Angle-integrated cross sections for electron-impact excitation of the $3p^54s$ states in argon from the $(3p^6)^1S_0$ ground state. The results from a variety of BSR models (see the text) are compared with each other to provide an indication of the convergence pattern in the theoretical predictions.

### B. Excitation

In this subsection we exhibit the angle-integrated cross sections for excitation of the $3p^54s$, $3p^54p$, $3p^53d$, and $3p^55s$ states over an extended energy range from threshold up to 300 eV. In addition to comparing our predictions with experimental data and a number of other calculations, we present a convergence study in order to provide an estimate about the reliability of the BSR results regarding the number of states included in the close-coupling expansion.

Figures 3 and 4 show results for excitation of the four states with principal configuration $3p^54s$. Starting with the convergence study (Fig. 3), we notice a very strong dependence of the theoretical results on the number of coupled states in the model. Keeping only the five states of interest (ground state plus the four excited states) produces results that are apparently far too large, especially in the intermediate-energy regime of incident energies between the ionization threshold and about five times this value. Increasing the number of coupled discrete states to 31 and 78, respectively, reduces the predicted peak and shifts it to larger energies. Only after including a significant number of additional pseudostates with energies in the ionization continuum, however, some convergence seems to have been established. A few checks with 600 (the maximum we can handle with current computational resources) rather than 500 states in the BSR expansion hardly produces any

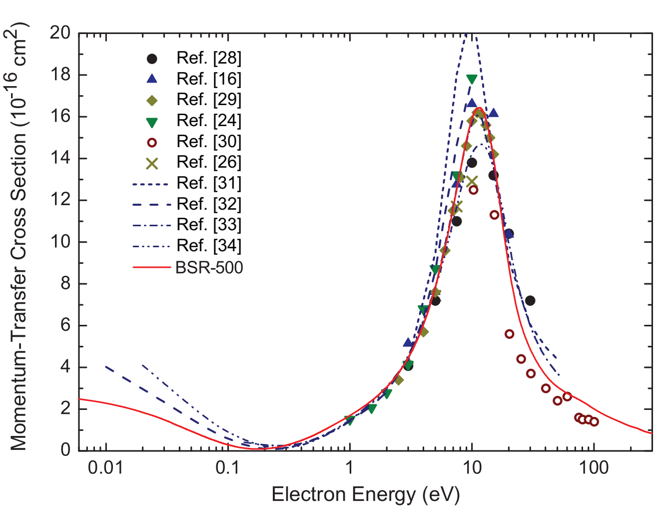


FIG. 2. (Color online) Momentum-transfer cross section for elastic electron scattering from argon atoms in their $(3p^6)^1S_0$ ground state. The current BSR-500 results are compared with a variety of experimental data [16,24,26,28–30] and predictions from other theoretical models [31–34] indicated in the legend.

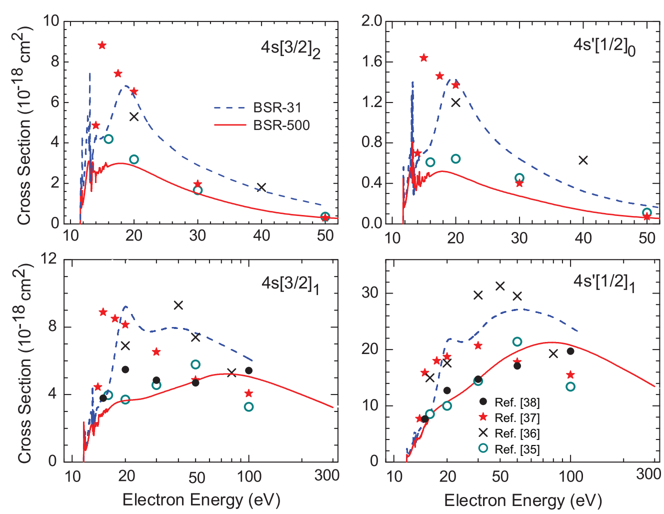


FIG. 4. (Color online) Angle-integrated cross sections for electron-impact excitation of the $3p^54s$ states in argon from the $(3p^6)^1S_0$ ground state. The current BSR-500 results are compared with those from a BSR-31 model, as well as experimental data from Chutjian and Cartwright [35], Filipović *et al.* [36], Khakoo *et al.* [37], and Hoshino *et al.* [38].

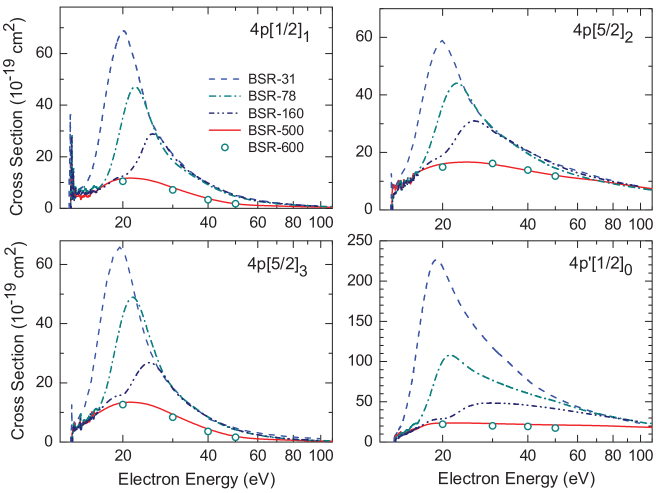


FIG. 5. (Color online) Angle-integrated cross sections for electron-impact excitation of the $3p^54p$ states in argon from the $(3p^6)^1S_0$ ground state. The results from a variety of BSR models (see the text) are compared with each other to provide an indication of the convergence pattern in the theoretical predictions.

further changes, thereby providing some confidence in the BSR-500 predictions.

The need for reliable data is further illustrated in Fig. 4. The available experimental data vary considerably. Interestingly, the oldest [35] and newest [38] data sets (the latter are only available for the optically allowed excitation of the $J = 1$ states) agree best with each other and also with the BSR-500 predictions.

Moving on to excitation of the $3p^54p$ states, the pattern is similar to that described for the $3p^54s$ manifold above. Including a large number of pseudostates is even more important in these cases (see Fig. 5). This is a typical finding for optically forbidden transitions and hence not surprising either. In fact, it was also seen in a purely nonrelativistic calculation performed by Ballance and Griffin [39]. Due to the mixing of $LS$ terms, however, no direct comparison with either experiment or our results is possible.

As seen from Fig. 6, the agreement between the available experimental data is, once again, by no means satisfactory. Given the systematic behavior of the theoretical predictions displayed in Fig. 5, as well as the quality of our target description, we believe that the BSR-500 results are well suited to be used as a consistent data set in plasma modeling applications.

The very same pattern continues for excitation of the $3p^53d$ states (Figs. 7 and 8) as well as the $3p^55s$ states (Fig. 9). The available experimental data become very scarce and the agreement with the BSR-500 prediction is far from perfect. Once again, we emphasize that the dependence of the BSR predictions as a function of collision energy and the number of states retained in the close-coupling expansion agrees with general expectations and previous findings for the neon target.

### C. Ionization and total cross sections

With the large number of pseudostates included in the BSR-500 model, it is also possible to extract results for ionization

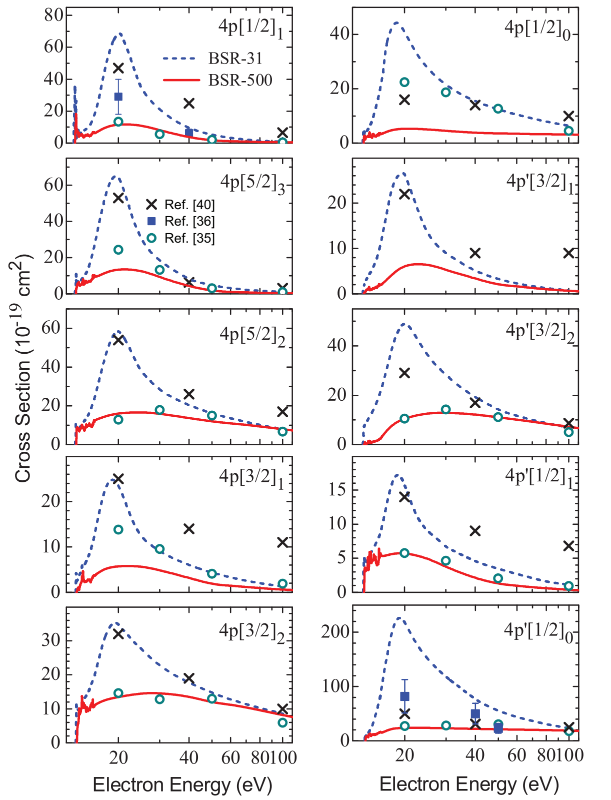


FIG. 6. (Color online) Angle-integrated cross sections for electron-impact excitation of the $3p^54p$ states in argon from the $(3p^6)^1S_0$ ground state. The current BSR-500 results are compared with those from a BSR-31 model, as well as experimental data from Chutjian and Cartwright [35], Chilton *et al.* [40], and Filipovic *et al.* [36].

of both the $(3p^6)^1S_0$ ground state (Fig. 10) and the metastable $(3p^54s)^3P_{2,0}$ states (Fig. 11). This is simply done by adding up the cross sections for all pseudostates with energy in the ionization continuum.

Figure 10 shows excellent agreement between the BSR-500 predictions and the most recent experimental data of Sorokin *et al.* [42] and Rejoub *et al.* [43] for incident energies between 100 and 200 eV. In contrast, our model does not reproduce the very rapid increase of the ionization cross section between threshold and about 40 eV, with a subsequent plateau in the experimental data of Rejoub *et al.* [43] between 40 and 100 eV. Interestingly, the predictions from the smaller nonrelativistic RMPS model of Ballance *et al.* [44] produce better agreement with experiment in the energy regime near the ionization threshold. Even though the calculation was limited to 50 eV, the trend suggests a likely overestimate of the ionization cross section above 50 eV, similar though probably not as pronounced as in the hybrid distorted-wave plus $R$-matrix model of Bartschat and Burke [45].

Results for ionization of the metastable $(3p^54s)^3P_{2,0}$ states are presented in Fig. 11. While, in contrast to all other theoretical results, the BSR-500 predictions are in excellent agreement with the experimental data of Dixon *et al.* [46] regarding the energy dependence of the cross section, they are smaller by about a factor of 0.65. We have no explanation for

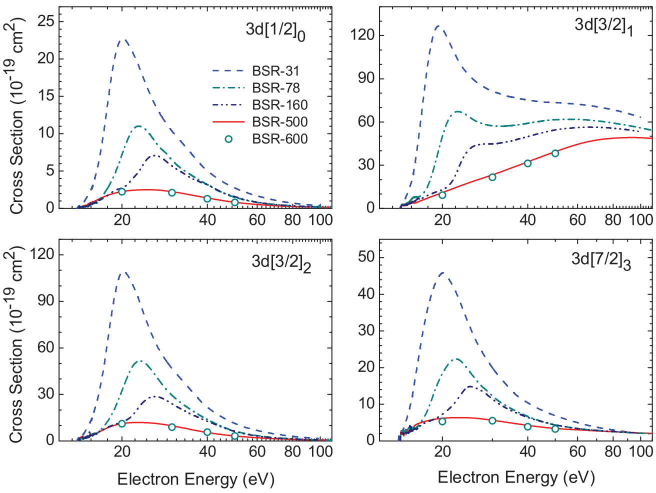


FIG. 7. (Color online) Angle-integrated cross sections for electron-impact excitation of the $3p^5 3d$ states in argon from the $(3p^6)^1S_0$ ground state. The results from a variety of BSR models (see the text) are compared with each other to provide an indication of the convergence pattern in the theoretical predictions.

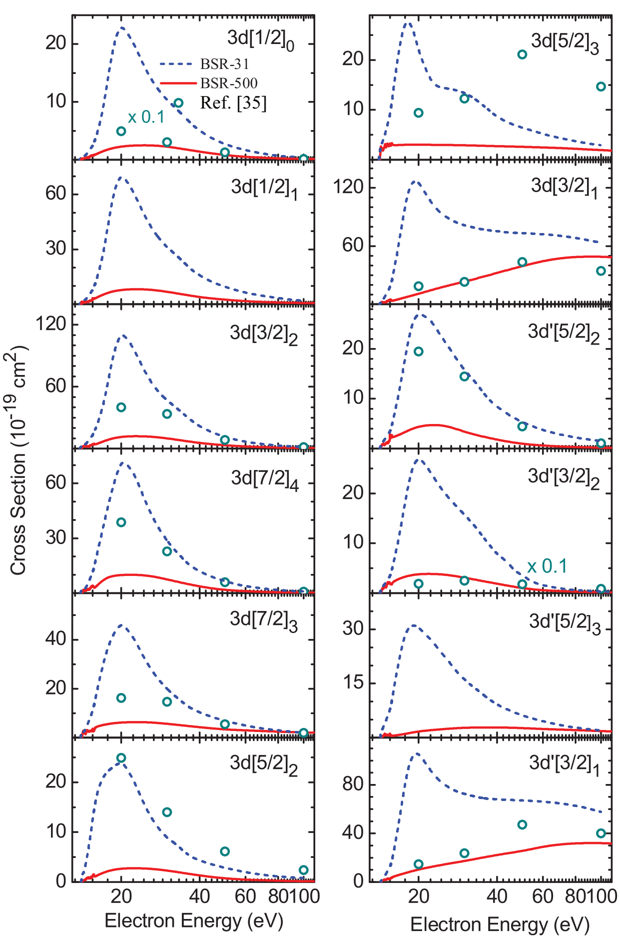


FIG. 8. (Color online) Angle-integrated cross sections for electron-impact excitation of the $3p^5 3d$ states in argon from the $(3p^6)^1S_0$ ground state. The current BSR-500 results are compared with those from a BSR-31 model as well as experimental data from Chutjian and Cartwright [35].

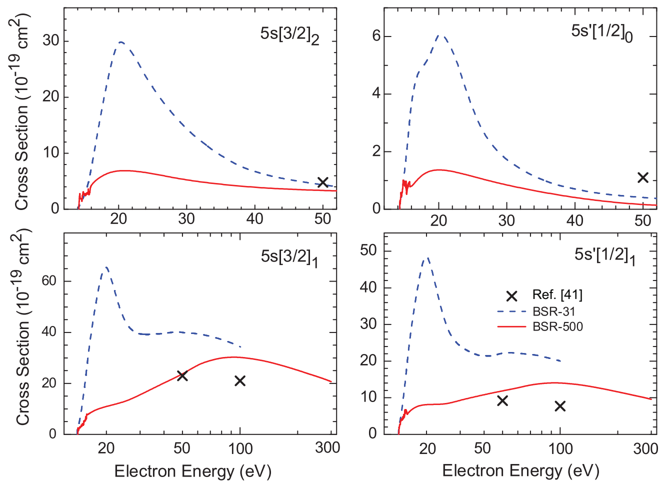


FIG. 9. (Color online) Angle-integrated cross sections for electron-impact excitation of the $3p^5 5s$ states in argon from the $(3p^6)^1S_0$ ground state. The current BSR-500 results are compared with those from a BSR-31 model as well as experimental data from Stewart *et al.* [41].

this result, but we note that a similar controversy exists between the experimental results of Dixon *et al.* [47] for ionization of the metastable $(1s2s)^3S$ state in helium, for which a number of very sophisticated theoretical methods predict results that agree within a few percent while they differ from experiment by about a factor of 2. Consequently, we concur with Fursa and Bray [48] that there has likely been a problem with the absolute normalization in the experiments of Dixon *et al.* [46,47].

We finish our presentation with the grand total cross section for electron collisions with argon atoms in their $(3p^6)^1S_0$ ground state, i.e., the sum of angle-integrated elastic,

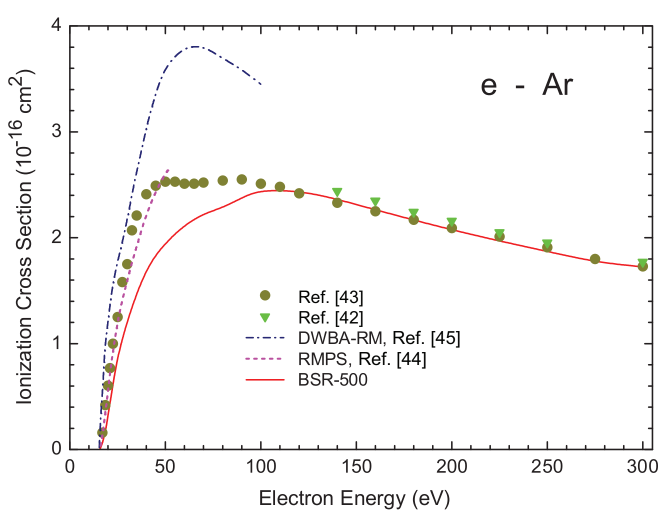


FIG. 10. (Color online) Angle-integrated cross sections for electron-impact ionization of the $(3p^6)^1S_0$ ground state of argon. The current BSR-500 results are compared with those from a hybrid distorted-wave Born approximation–$R$-matrix (DWBA-RM) model [45] and a standard nonrelativistic RMPS approach [44], as well as experimental data from Sorokin *et al.* [42] and Rejoub *et al.* [43].

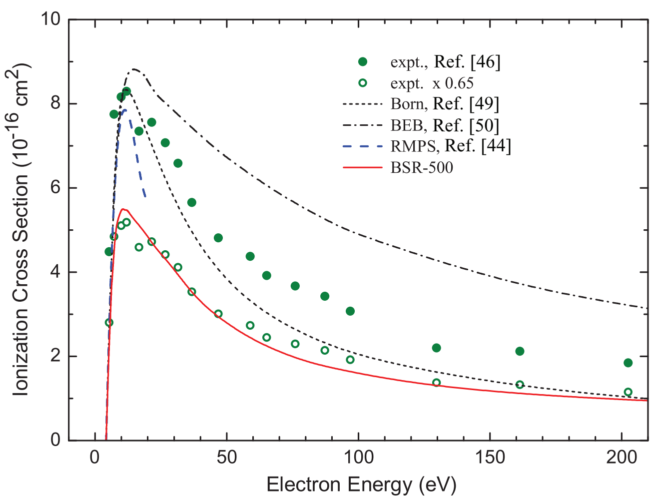


FIG. 11. (Color online) Angle-integrated cross sections for electron-impact ionization of the $(3p^5 4s)^3P_{2,0}$ metastable states of argon. The current BSR-500 results are compared with those from a first-order Born model [49], a binary-encounter Bethe model [50], a standard nonrelativistic RMPS approach [44], and the experimental data of Dixon *et al.* [46]. In order to show the excellent agreement in the predicted energy dependence, the experimental data are also presented after rescaling by a factor of 0.65.

excitation, and ionization cross sections. The BSR-500 results are displayed in Fig. 12. While the elastic cross section provides the largest contribution over the energy range shown, ionization becomes almost equally important at 200 eV and above, while excitation processes represent about 10% of the grand total cross section. Since the momentum-transfer rather than the elastic cross section is typically important for plasma modeling, it is also presented in Fig. 12. The difference between the two cross sections is substantial and hence the elastic cross section is not recommended as a substitute in case the momentum-transfer result is not available.

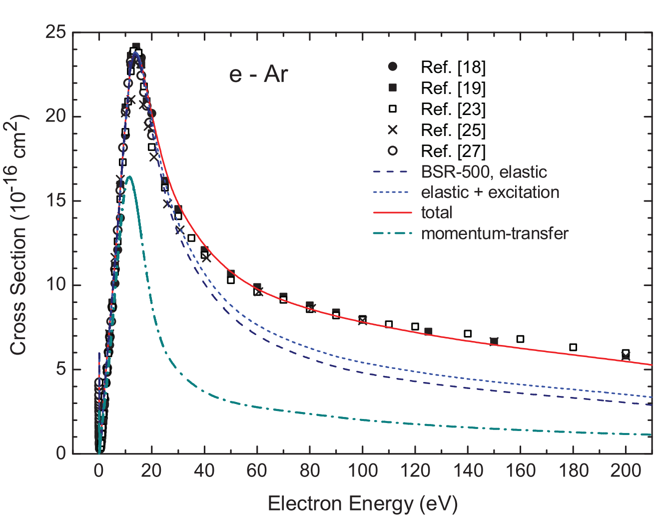


FIG. 12. (Color online) Angle-integrated grand total cross section for electron collisions with argon atoms in their $(3p^6)^1S_0$ ground state. The current BSR-500 results are compared with a variety of experimental data [18,19,23,25,27]. Also shown are the contributions from elastic scattering alone and elastic scattering plus excitation processes, as well as the momentum-transfer cross section.

### D. Interpretation of the results

After presenting the numerical results, which clearly exhibit some systematic behavior, we will now attempt to provide some *qualitative* explanation for what we see. It is well known that the elastic cross section, both angle-integrated and angle-differential, is relatively stable with respect to changes in a theoretical model. Especially for scattering near the forward direction, the most important ingredient in a model is the dipole polarizability. The latter is determined by the oscillator strengths to all the states connected to the initial state.

There are several important consequences from this result. (1) If one of the transitions dominates, e.g., $n\,^2S \rightarrow n\,^2P^o$ in alkali-metal atoms, the convergence of the close-coupling expansion is fast, i.e., coupling just a few states (sometimes only the two mentioned above) may give very satisfactory results. A well-known example is the classic paper by Moores and Norcross [51] on electron-Na collisions. (2) In contrast, if the contributions to the dipole polarizability are spread out and a significant fraction even comes from coupling to the ionization continuum (as generally happens when moving across the columns of the periodic table from the alkali metals to the noble gases), the convergence slows down. This is effectively what we see for the present case of interest, electron-Ar collisions. (3) Nevertheless, even in the latter case, the predicted elastic cross section is relatively insensitive to the number of states included.

The optical theorem (see any textbook on quantum scattering phenomena), which connects the imaginary part of the elastic scattering amplitude to the grand total cross section via the simple factor of $4\pi/k$ (where $k$ is the magnitude of the indent projectile momentum), is essentially the reason why the elastic and the grand total cross sections are relatively straightforward to obtain in a numerical calculation. The difficulty, however, lies in the decomposition of the inelastic (grand total minus elastic) cross section. If only a few discrete states are included in the close-coupling expansion, the entire inelastic cross section in this unitary theory is made up from excitation of these few states. Hence, these excitation cross sections will likely be overestimated. If more and more discrete states are included, the individual cross sections for the few states selected earlier will likely go down (assuming that the total inelastic cross section is fairly stable) and they will go down further if coupling to the ionization continuum is accounted for. Since ionization is such an important process in the problem at hand (see Fig. 12), it is ultimately not surprising that the effect of overestimating the discrete excitation cross sections is so dramatic in the current problem.

While only a qualitative explanation, it describes the general pattern seen not only in this calculation, but in many others carried out before. The details depend on the particular target, the transition of interest, and the collision energy. This fact continues to make energetic electron scattering a serious challenge to quantum collision theory due to the infinite number of states that are either energetically accessible (above the ionization threshold) or may affect the results via (closed-)channel coupling.

## IV. CONCLUSION

We employed a recently developed parallel version of the BSR suite of computer programs [14] to carry out large-scale $R$-matrix-with-pseudostates calculations for electron scattering from argon atoms. These calculations were performed in the intermediate-coupling scheme and hence provide individual state-to-state results for excitation.

Our results support earlier predictions [39,52] (already confirmed for electron-Ne collisions in [6,7]) regarding a very strong influence of coupling to the target continuum in calculating excitation cross sections, in particular when the active electron is promoted to the $3d$ orbital. This sensitivity seems to be a general trend, as it is also seen in recent calculations for electron-C [53] and electron-Si [54] collisions.

The results reported in this paper are available in electronic format upon request. We believe that these cross sections considerably improve and extend the existing database for electron-Ar collisions. Given the remaining discrepancies with absolute experimental data for some excitation cross sections, further measurements with accurate absolute normalization are highly desirable. Similarly extensive calculations for electron collisions with Kr and Xe atoms are left for future work. The latter will require a parallelized fully relativistic version of the BSR codes.

## ACKNOWLEDGMENTS

We thank Leanne Pitchford for many discussions regarding our calculations. This work was supported by the United States National Science Foundation under Grants No. PHY-0903818 and No. PHY-1212450 and by the XSEDE supercomputer allocation No. PHY-090031. The calculations were carried out on Stampede at the Texas Advanced Computing Center and Gordon at the San Diego Supercomputer Center. Y.W. was sponsored by the China Scholarship Council and would like to thank Drake University for hospitality during his visit.


[1] L. C. Pitchford, L. L. Alves, K. Bartschat, S. F. Biagi, M. C. Bordage, A. V. Phelps, C. M. Ferreira, G. J. M. Hagelaar, W. L. Morgan, S. Pancheshnyi, V. Puech, A. Stauffer, and O. Zatsarinny, J. Phys. D **46**, 334001 (2013).

[2] L. L. Alves, M. C. Bordage, S. F. Biagi, L. C. Pitchford, O. Zatsarinny, K. Bartschat, G. J. M. Hagelaar, S. Pancheshnyi, C. M. Ferreira, V. Puech, W. L. Morgan, and A. V. Phelps, J. Phys. D **46**, 334002 (2013).

[3] M. C. Bordage, S. F. Biagi, L. C. Pitchford, K. Bartschat, S. Chowdhury, G. J. M. Hagelaar, W. L. Morgan, V. Puech, and O. Zatsarinny, J. Phys. D **46**, 334003 (2013).

[4] K. Bartschat, J. Phys. D **46**, 334004 (2013).

[5] http://nl.lxcat.net/home/

[6] O. Zatsarinny and K. Bartschat, Phys. Rev. A **85**, 062710 (2012).

[7] O. Zatsarinny and K. Bartschat, Phys. Rev. A **86**, 022717 (2012).

[8] O. Zatsarinny and C. Froese Fischer, Comput. Phys. Commun. **180**, 2041 (2009).

[9] O. Zatsarinny and K. Bartschat, Phys. Scr. **T134**, 014020 (2009).

[10] O. Zatsarinny and K. Bartschat, J. Phys. B **37**, 4693 (2004).

[11] A. Kramida, Yu. Ralchenko, J. Reader *et al.*, NIST Atomic Spectra Database, Version 5, http://www.nist.gov/pml/data/asd.cfm (National Institute of Standards and Technology, Gaithersburg, 2012).

[12] Z. P. Zhong, S. L. Wu, R. F. Feng, B. X. Yang, Q. Ji, K. Z. Xu, Y. Zou, and J.-M. Li, Phys. Rev. A **55**, 3388 (1997).

[13] D. R. Johnston, G. J. Oudemans, and R. H. Cole, J. Chem. Phys. **33**, 1310 (1960).

[14] O. Zatsarinny, Comput. Phys. Commun. **174**, 273 (2006).

[15] N. Badnell, J. Phys. B **32**, 5583 (1999); see also http://amdpp.phys.strath.ac.uk/UK_RmaX/codes.html

[16] S. K. Srivastava, H. Tanaka, A. Chutjian, and S. Trajmar, Phys. Rev. A **23**, 2156 (1981).

[17] K. Jost, P. G. F. Bisling, F. Eschen, M. Felsmann, and L. Walther, in *XIII International Conference on the Physics of Electronic and Atomic Collisions, Abstracts of Contributed Papers*, edited by J. Eichler, W. Fritsch, I. V. Hertel, N. Stolterfoht, and U. Wille (North-Holland, Amsterdam, 1983), p. 91.

[18] J. Ferch, B. Granitza, C. Masche, and W. Raith, J. Phys. B **18**, 967 (1985).

[19] J. C. Nickel, K. Imre, D. F. Register, and S. Trajmar, J. Phys. B **18**, 125 (1985).

[20] K. P. Subramanian and V. Kumar, J. Phys. B **20**, 5505 (1987).

[21] S. J. Buckman and B. Lohmann, J. Phys. B **19**, 2547 (1986).

[22] J. E. Furst, D. E. Golden, M. Mahgerefteh, J. Zhou, and D. Mueller, Phys. Rev. A **40**, 5592 (1989).

[23] C. Szmytkowski and K. Maciag, Phys. Scr. **54**, 271 (1996).

[24] J. C. Gibson, R. J. Gulley, J. P. Sullivan, S. J. Buckman, V. Chan, and P. D. Burrow, J. Phys. B **29**, 3177 (1996).

[25] W. Y. Baek and B. Grosswendt, J. Phys. B **36**, 731 (2003).

[26] B. Mielewska, I. Linert, G. C. King, and M. Zubek, Phys. Rev. A **69**, 062716 (2004).

[27] M. Kurokawa, M. Kitajima, K. Toyoshima, T. Kishino, T. Odagiri, H. Kato, M. Hoshino, H. Tanaka, and K. Ito, Phys. Rev. A **84**, 062717 (2011).

[28] L. S. Frost and A. V. Phelps, Phys. Rev. **136**, A1538 (1964).

[29] Y. Nakamura and M. Kurachi, J. Phys. D **21**, 718 (1988).

[30] R. Panajotović, D. Filipović, B. Marinković, V. Pejĉev, M. Kurepa, and L. Vusković, J. Phys. B **30**, 5877 (1997).

[31] R. P. McEachran and A. D. Stauffer, J. Phys. B **16**, 4023 (1983).

[32] R. P. McEachran and A. D. Stauffer, Aust. J. Phys. **50**, 511 (1997).

[33] A. Dasgupta and A. K. Bhatia, Phys. Rev. A **32**, 3335 (1985).

[34] K. L. Bell, N. S. Scott, and M. A. Lennon, J. Phys. B **17**, 4757 (1984).

[35] A. Chutjian and D. C. Cartwright, Phys. Rev. A **23**, 2178 (1981).

[36] D. M. Filipović, B. P. Marinković, V. Pejčev, and L. Vušković, J. Phys. B **33**, 2081 (2000).

[37] M. A. Khakoo, P. Vandeventer, J. G. Childers, I. Kanik, C. J. Fontes, K. Bartschat, V. Zeman, D. H. Madison, S. Saxena, R. Srivastava, and A. D. Stauffer, J. Phys. B **37**, 247 (2004).

[38] M. Hoshino, H. Murai, H. Kato, Y. Itikawa, M. J. Brunger, and H. Tanaka, Chem. Phys. Lett. **585**, 33 (2013).

[39] C. P. Ballance and D. C. Griffin, J. Phys. B **41**, 065201 (2008).
[40] J. E. Chilton, J. B. Boffard, R. S. Schappe, and C. C. Lin, Phys. Rev. A **57**, 267 (1998).
[41] M. D. Stewart, Jr., J. E. Chilton, J. B. Boffard, and C. C. Lin, Phys. Rev. A **65**, 032704 (2002).
[42] A. A. Sorokin, L. A. Shmaenok, S. V. Bobashev, B. Möbus, M. Richter, and G. Ulm, Phys. Rev. A **61**, 022723 (2000).
[43] R. Rejoub, B. G. Lindsay, and R. F. Stebbings, Phys. Rev. A **65**, 042713 (2002).
[44] C. P. Ballance, D. C. Griffin, M. S. Pindzola, and S. D. Loch, J. Phys. B **40**, F27 (2007).
[45] K. Bartschat and P. G. Burke, J. Phys. B **21**, 2969 (1988).
[46] A. J. Dixon, M. F. A. Harrison, and A. C. H. Smith, in *VIII International Conference on the Physics of Electronic and Atomic Collisions, Abstracts of Contributed Papers*, edited by B. C. Cobic and M. V. Kurepa, Vol. 1 (Institute of Physics, Belgrade, 1973), p. 405.
[47] A. J. Dixon, M. F. A. Harrison, and A. C. H. Smith, J. Phys. B **9**, 2617 (1976).
[48] D. V. Fursa and I. Bray, J. Phys. B **36**, 1663 (2003).
[49] D. Ton-That and M. R. Flannery, Phys. Rev. A **15**, 517 (1977).
[50] M. A. Ali and P. M. Stone, Int. J. Mass Spectrom. **271**, 51 (2008).
[51] D. L. Moores and D. W. Norcross, J. Phys. B **5**, 1482 (1972).
[52] C. P. Ballance and D. C. Griffin, J. Phys. B **37**, 2943 (2004).
[53] Y. Wang, O. Zatsarinny, and K. Bartschat, Phys. Rev. A **87**, 012704 (2013).
[54] V. Gedeon, S. Gedeon, V. Lazur, E. Nagy, O. Zatsarinny, and K. Bartschat, Phys. Rev. A **85**, 022711 (2012).